

An Attempt to Analyze the Influence of Properties of Five African Wood Species on Cemented Carbide Tool Wearing

Bolesław Porankiewicz,^{a,*} Daria Wieczorek,^b Anita Bocho-Janiszewska,^c and Emilia Klimaszewska^c

The dulling of cemented carbide cutting tools after milling five African wood species was studied. The wood specimens investigated varied in high temperature corrosivity (HTC), hard mineral contamination (HMC), and density (*D*). Attempts to replace the combustion method of evaluating the content of natural HMC in wood with spectral mass analysis methods, such as energy dissipative spectrum (EDAX) or atomic absorption spectrometry (AAS), failed. Experiments showed that scanning electron microscope (SEM) analysis of the ash yielded information on the size and shape of small-dimension, natural HMC particles present in the wood specimens. Employing theoretical multi-variable simulation, the combined effects of the HTC, the HMC, and the *D* on the cemented carbide tool wear was modeled and appeared to be a good explanation of the results observed.

Keywords: Cemented carbide tool; Wearing; Milling; African Wood Species; Hard mineral contamination; High temperature corrosivity; Wood density

Contact information: a: Poznań University of Technology, Piotrowo 5, 60-450 Poznań, Poland; b: Department of Technology and Instrumental Analysis, Poznań University of Economics, al. Niepodległości 10, 61-875 Poznań; c: Department of Chemistry, University of Technology and Humanities in Radom 26-600 Radom, ul. Chrobrego 27, Poland; *Corresponding author: poranek@amu.edu.pl

INTRODUCTION

Previous studies have reported that the machining of some tropical wood species in a dry state excessively dulls high speed steel (HSS) cutting tools (Porankiewicz *et al.* 2003, 2006; Porankiewicz *et al.* 2008). This phenomenon was explained to be a result of synergistic effects of mechanical wear (abrasion) caused by the hard mineral contamination (HMC) and high temperature corrosivity (HTC). Chemical and mechanical wearing of the HSS and the cemented carbide tools by tropical wood machining was also the subject of work by Darmawan *et al.* (2006), but no HTC was considered in that work. The synergistic effect also explained the high tool wear observed in the case of wood with low HMC and high HTC. The effect of wood density was of lesser importance. In recent works by Cristóvão *et al.* (2009; 2010), studies of the wear of cemented carbide cutting tools when milling low- and high-density, dry, tropical African wood species was examined. Several issues discussed in these works are controversial. In the opinion of the authors of this study, cutting tool wearing when machining wood in the dry state versus in the green state is markedly different. Examining the role of extracts in the case of dry wood cutting experiments has limited value. Similarly, in conducting wearing experiments with dry, solid wood, it is inappropriate to quote studies of cutting tool dulling where green wood or fiber and particle board is cut and machined (in a dry state). The authors' previous findings,

from Porankiewicz (2003a,b) and Porankiewicz *et al.* (2006, 2008), state that the basic wear mechanism on dry wood and secondary wood products machining is the combined effects of the HMC and the HTC, whereas when cutting wood in the green state, wet corrosion is of the greatest importance for some wood species and tool materials.

Another controversial issue that should have been mentioned in recent works (Cristóvão *et al.* 2009, 2010) relates to the cutting tool dullness parameters chosen for wearing experiments. Several parameters for the determination of tool bluntness have been used by researchers because of the irregularity of the real edge round up. In the case of machining solid wood by low HMC and with low HTC, a radius of edge round up, ρ , measured on a plane perpendicular to the edge, seems sufficient. In this case, the edge recession is regular and is the same along the rake, A_γ , and the clearance surface, A_α . In the case of presence of HMC and HTC, edge recession along the clearance face VB_F is usually larger, so this parameter should be chosen. In this case, an average value of the ρ must be evaluated. In the case of edge chipping, the parameter describing the largest edge wear should be measured. Parameters based on the area of edge wear measured in any plane provide averaged information useless from the point of view of acceptable machining quality and the corresponding edge dullness (Staniszewski and Porankiewicz 1978; Porankiewicz 2014).

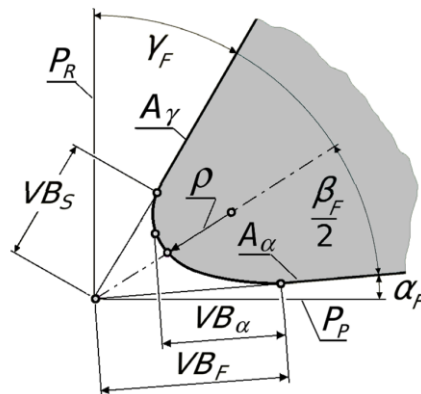


Fig. 1. Parameters describing edge dullness after cutting solid wood containing HMC; P_R - Main plane; P_P - Back plane; A_γ - rake face; A_α - clearance face; γ_F - contour rake angle; α_F - contour clearance angle; β_F - contour sharpness angle; ρ - edge round up; VB_S - edge recession along the A_γ ; VB_α - flank wear; VB_F - edge recession along the A_α

The next controversial issue presented in recent works (Cristóvão *et al.* 2009, 2010) relates to an acceptable content of the HMC. In the case of solid wood from a hot, tropical climate, the term “acceptable HMC” does not seem useful; however, the term “acceptable HMC” is otherwise important in the case of particle and fiber boards because the HTC can be reduced by the modernization of technological processes.

A very important issue related to the influence of the HMC on tool wearing is the size of contaminant particles. This issue has been omitted from many works (Cristóvão *et al.* 2009, 2010), although the effect of the size of HMC particles on tool wear during solid wood milling has already been reported (Porankiewicz *et al.* 2003, 2006; Porankiewicz 2008).

The present work is an attempt to analyze cemented carbide tool wearing after the longitudinal milling of five tropical wood species originating from Mozambique.

EXPERIMENTAL

Experiments were performed using an SCM milling machine at Luleå University of Technology, Wood Technology Faculty Skellefteå, according to the works of Cristóvão *et al.* (2009, 2010) using the following machining parameters: rotational speed, $n = 2900 \text{ min}^{-1}$; diameter of cutter head, number of cutting edges $z = 1$, $D_{CH} = 154 \text{ mm}$; feed speed, $v_F = 3 \text{ m/min}$; depth of cut, $c_d = 1 \text{ mm}$; cutting length per cut, $l_C = 12.41 \text{ mm}$; cutting width, $w_C = 3.9 \text{ mm}$; rake angle, $\gamma_F = 30^\circ$; and clearance angle, $\alpha_F = 15^\circ$. Up-milling of the longitudinal cutting case was used and had an edge orientation angle of $\varphi_E = 90^\circ$ and average vector of the cutting speed and cutting plane orientation angles $\varphi_V = \varphi_S = 9.24^\circ$. The average moisture content was $m_C = 8$ to 9% .

The cutting blade was made of grade 701 cemented carbide provided by Sandvik Hard Materials Company (Sweden). This grade contains 89.5% tungsten carbide (WC), 10% cobalt (Co), and 0.5% other compounds. The Vickers hardness of the cutting blade material was 1600 HV_{30} , and the Rockwell hardness was 92.1 HRA. The wood specimens examined in the present study are listed in Table 1 and shown in Fig. 2.

Table 1. Wood Specimens Used in the Experiment

no.	Common name	Scientific name	Wood density (kg/m^3)
1	Ntholo	<i>Pseudolachnostylis maprounaefolia</i>	726
2	Namuno	<i>Acacia nigrescens</i>	1100
3	Muanga	<i>Pericopsis angolensis</i>	920
4	Metil	<i>Sterculia appendiculata</i>	550
5	Iron wood	<i>Swartzia madagascariensis</i>	1100

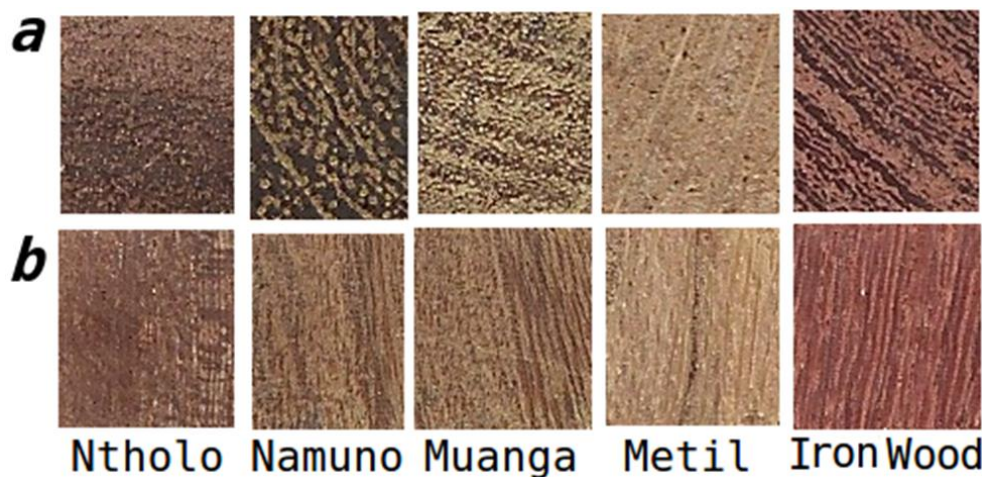


Fig. 2. Sections in direction towards wood grains of specimens examined: a - perpendicular; b - parallel

The content of the HMC, C_{MC} , (mainly silica based compounds), and content of the ash, in the wood specimens were evaluated using a combustion method. The oven-dry wood specimens of weight of about 1 g were dried to absolute dry state in a chamber dryer in temperature $105 \text{ }^\circ\text{C}$, then cooled down in an exsiccator and weighted before burning with accuracy of 0.0001 g. For evaluation of the HMC, the ash was etched 30 min in hot hydrochloric acid and filtered with use of the Whatman glass filters. After filtering, the

glass filters were washed in distilled water and dried out in a chamber dryer. The difference of the mass of dry glass filters after and before filtering was the amount of the HMC. The content of the HMC and content of the ash were related to absolute dry wood specimens before burning. In order to characterize the size, S_{MC} , of the HMC particles, 4 fractions (used in previous experiments) were assumed: $f_1 <0; 50>$, average 25 μm ; $f_2 <50; 75>$, average 63 μm ; $f_3 <75; 100>$, average 88 μm ; $f_4 <100; 200>$, average 150 μm . The size was an average value from maximum and minimum dimensions of particles measured on a scanning electron microscope (SEM) images of Whatman glass filters. The ash was examined, with regards to the size and shape of the HMC particles, using SEM, type FEI Quanta 250 FEG, in a low pressure mode (110 Pa). The ash was also analyzed, with regard to its chemical composition, using an energy dissipative spectrometer EDAX type Genesis XM 2i equipped with a nitrogen-free EDAX Apollo 10 detector.

Thermogravimetric analysis (TGA) was used to evaluate the HTC of the products of the thermal degradation of wood towards *Co* and iron (*Fe*), the binders of the tool materials. TGA was repeated twice for each wood specimen. The conditions of the analysis, which was performed with a Shimadzu TGA-50 apparatus, were as follows: free flow of ambient air; up to 650 $^{\circ}\text{C}$; heating rate of 50 $^{\circ}\text{C}/\text{min}$; platinum crucible; proportion of *Co* and *Fe* and wood powders was 17 to 20 mg and 1 to 2 mg, respectively; and smoothing filter in TASY Software 40. The most important part of the method of evaluating the HTC using the Shimadzu TGA-50 apparatus was the unbalanced magnetic field (as high as $2.5 \cdot 10^{-4} \text{ N}/(\text{A} \cdot \text{m})$, at 50 Hz) inside the oven. The HTC peak on the TGA plot is shown in Fig. 3.

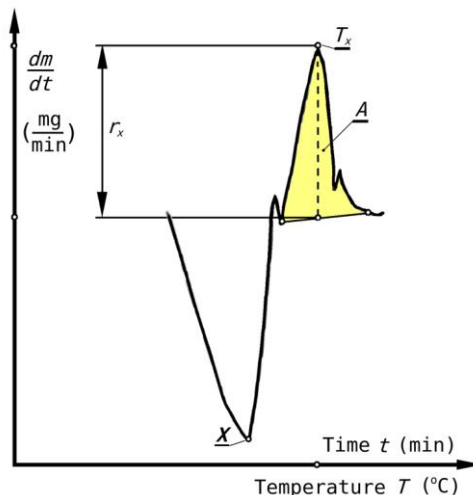


Fig. 3. Parameters of the corrosion peak used for calculations of the quantifier, R_x ; dm/dt – first derivative of mass, m , against time, t ; r_x – height of corrosion peak; T_x – temperature of maximum corrosion peak; A – area of corrosion peak

The HTC quantifier was calculated using Eq. 1 as the average from two replicate TGA analyses. According to a previous work (Porankiewicz 2008), small peaks were ignored in the evaluation of the HTC quantifier, R_x ,

$$R_x = r_x / m \quad (\text{min}^{-1}) \quad (1)$$

where r_x is the maximum height of the corrosion peak after maximum degradation of mass (point X in Fig. 3) of the wood specimen (mg/min) and m is the mass of the metal specimen (mg).

According to the functional spectral signature method, carbonyl powder particles of *Co* and *Fe* were approximately 2.5 μm in diameter. More details regarding the methodology of the HTC evaluation were described in an earlier work (Porankiewicz 2003b).

The edge recession along the clearance surface, VB_F (Fig. 1) and the edge round up, ρ , were evaluated in the works of Cristóvão *et al.* (2009, 2010) using a light microscope (LM) and are collected in Table 2. A way of evaluating (minimum or average value) of the ρ was not explained in the works quoted. According to Fig. 4, the flank wear, VB_{α}^O , which is an approximation of edge abrasion on the clearance surface (Fig. 1), because the clearance surface of the blades was not precisely oriented perpendicularly to the optical axis of the microscope, was evaluated.

It must be noted that the choice to use a LM to measure the tool wear parameters, in the case of presence of HMC in the machined wood, is improper because the blade surfaces can be polished at some distance without measurable abrasion (on the order of a hundredth of a micron). The use of contact methods would be more suitable (with the application of a profilograph meter or replica method).

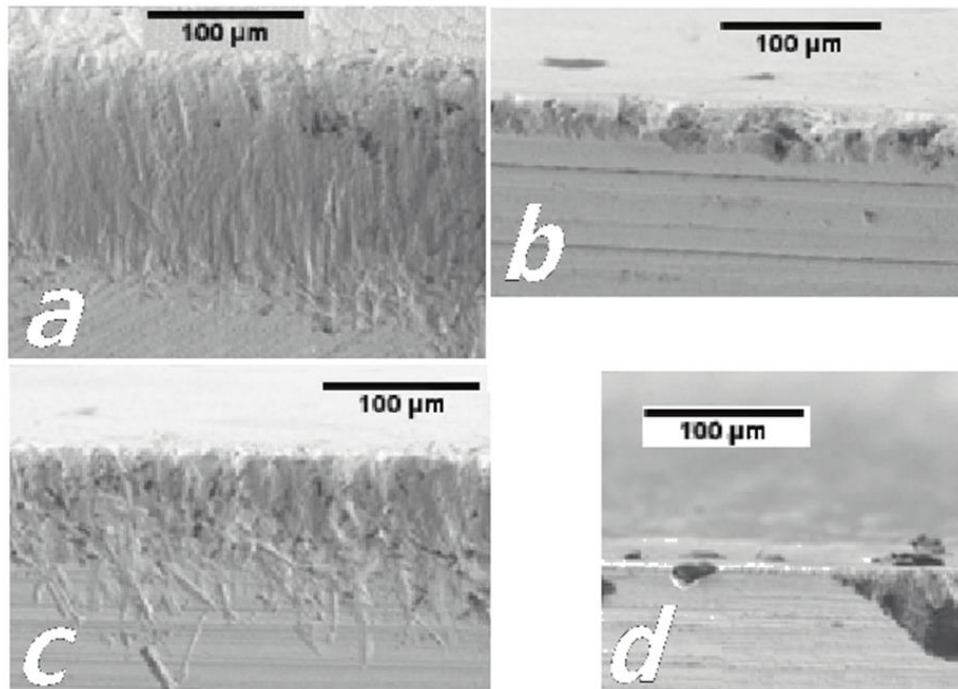


Fig. 4. LM images of the clearance surface of edges after cutting wood specimens: *a* – Ntholo, *b* – Namumo, *c* – Muanga, and *d* – Metil, according to Cristóvão *et al.* (2010)

Numerical analysis of the experimental data collected in Table 2 (ρ^O and VB_{α}^O) was performed at the Poznań Supercomputing and Networking Center (PCSS) on a heterogeneous, hybrid computing cluster GPGPU (67x Supermicro H8DGG and 42x Supermicro X9DRT) using an algorithm based on the modified theoretical simulation method developed by Porankiewicz (2008). The quality of the approximation provided by the theoretical simulation was characterized by the summation of the square residuals, S_R , as well as the square of the correlation coefficient, R^2 .

Table 2. Radius of Edge Round Up, ρ , and Edge Recession, VB , of Cemented Carbide 701 Edge, Before Machining (ρ_B , VB_{FB}) and Observed (ρ^O , VB_{α}^O) after Cutting Path, CP

Species no.	C_P	ρ_B	ρ^O	VB_{FB}	VB_{α}^O	VB_{FC}^C
	(m)	(μm)				
1. Ntholo	4896	2*	43	5 ²	140	93
2. Namuno	4896	2*	9	5 ²	28	55
3. Muanga	4896	2*	15	5 ²	70	50
4. Metil	4896	2*	5	5 ²	46	46
5. Iron Wood	2016 ¹	2 ¹	8 ¹	5 ²	20 ²	20 ²

Note: VB_{α} - flank wear; ¹ - values taken from work of Cristovao *et al.* (2009); * - assumed; ² - calculated; VB_{FC} - values of edge recession measured on the clearance surface, taken from the work of Cristóvão *et al.* (2011)

The synergistic effect, SE , was calculated as,

$$SE = (W_x - W_i) / W_x \quad (2)$$

where W_x is the maximum tool wear (ρ^O or VB_{α}^O) by the highest value of the C_{MC} and the largest value of the relatively HTC quantifier R_W and W_i is the tool wear (ρ^O or VB_{α}^O) by the minimum values of the C_{MC} and the minimum values of the relative HTC quantifier, R_W .

RESULTS AND DISCUSSION

In Fig. 5 can be seen as rounded, silica based particles of the HMC, recognized with use of EDAX analysis. Measurements performed showed that most of particles were smaller than 50 μm and can be assigned as “fraction 1” (Table 3).

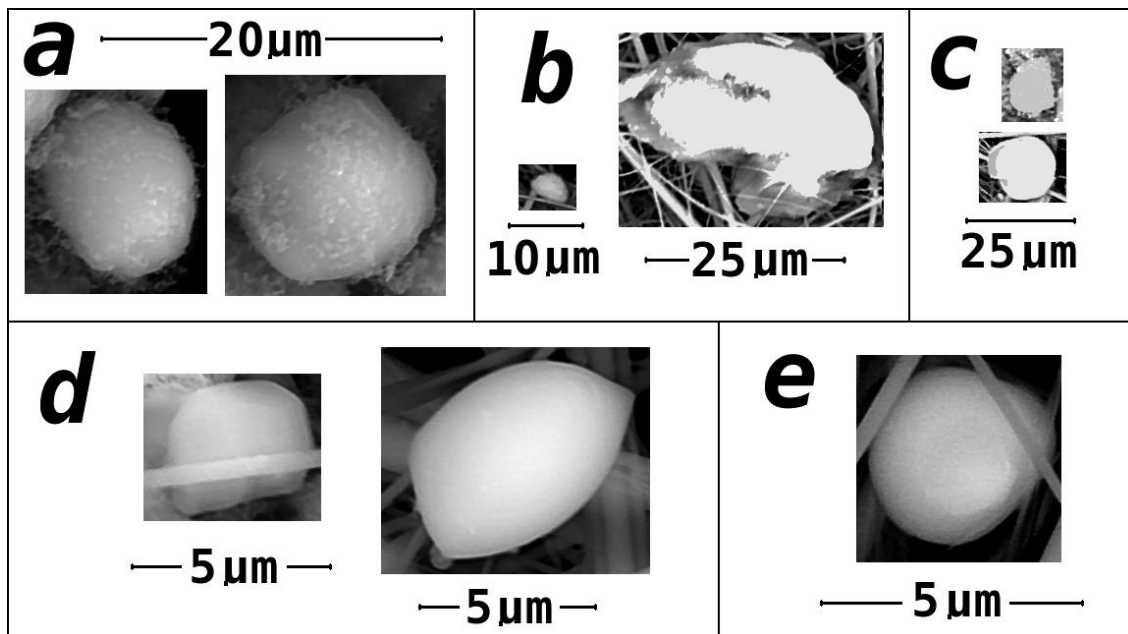


Fig. 5. Images of the HMC particles found on glass Whatman filters for: a - Ntholo, b – Namuno, c – Muanga, d – Metil, e – Iron wood; SEM

Measurements performed on SEM images and on the glass filters showed that the silica-based particles were smaller than 50 μm in size and can thus be designated as “fraction 1” (Table 3). Small HMC particles on the glass filters were not as easily visible as those in the SEM images. For one Muanga wood specimen, one larger particle was found and measured (on the glass filter) and was assigned to fraction 4. Table 3 contains information on C_{MC} and S_{MC} of the HMC and the HTC for all wood species examined. Wood specimen 1 (Ntholo), having $C_{MC} = 14524$ mg/kg, was the most mineral-contaminated of all specimens examined. The contents of the HMC in wood specimens 2, 3, 4, and 5 were much smaller (Table 3), especially that of specimen 2.

Table 3. Content of the HMC, C_{MC} , and Size, S_{MC} , of Contamination Particles; Ash Content; and HTC Quantifiers R_x and R_w for Co and the Fe Particles for the Wood Specimens Analyzed

no.	Common name	C_{MC} mg/kg	S_{MC}	Ash %	Co R_x min^{-1}	Co R_w	Fe R_x min^{-1}	Fe R_w
1	Ntholo	14524	f_1	6.27	0.0221	3.643	0.065	1.0
2	Namuno	723	f_1	1.54	0.029	5.09	0.1052	1.619
3	Muanga	2393	0.002 f_1 ; 0.998 f_4	2.19	0.0158	2.77	0.1024	1.576
4	Metil	2525	f_1	8.34	0.0057	1.0	0.1031	1.787
5	Iron wood	1865	f_1	0.89	0.0153	2.69	0.0904	1.392

The ash content in the wood specimens, evaluated using the combustion method, differed very much from that used in the work of Cristóvão *et al.* (2010). For the Ntholo and Metil wood specimens, the relative ash contents differed by about 2 times. Results of the EDAX analysis, as shown in Table 4, show that the largest silica content (Si) was found in specimen 1, in agreement with the results of the combustion analysis. A small presence of Si was confirmed in specimen 5. The presence of Si was not confirmed by the EDAX analysis in specimens 2, 3, or 4, which contradicts the results of the combustion analysis. The HMC content, which used to be associated with the silica content in wood specimens evaluated in the present study, with the use of combustion analysis, was much higher than one evaluated in the work of Cristóvão *at al.* (2010) with the application of the AAS method. The relative difference for the Ntholo wood specimen was a factor of 6.

Table 4. Results of EDAX Analysis of Ashes Remaining after Burning the Wood Specimens

Species no. and Name	Ca	K	Si	Mg	Al	Na	P	S
	(wt. %)							
1. Ntholo	37.3	1.7	1.0	2	0	0	0	0
2. Namuno	34.9	12.8	0	4.1	2.2	4.1	0	0
3. Muanga	25.1	29.8	0	5.3	1	0	0	0
4. Metil	16.8	29.1	0	7.4	0	0	3.1	0.7
5. Iron wood	27.8	2.2	1.1	11.6	1.1	0	0	1.7

For Muanga and Metil specimens, the relative values differed by factors of three and four, respectively. Spectroscopy methods such as the EDAX and AAS seemed unsuitable for evaluating the HMC content of wood specimens. The EDAX analysis (Table 4) also showed that calcium (Ca) was the main element present in the ash of wood specimens 1, 2, and 5. In wood specimens 3 and 4, more potassium (K) was found than Ca .

In the ash of all wood specimens, the presence of magnesium (*Mg*) was found, with the highest amount of 11.6 % found in specimen 5. No relationship between the amount of elements shown in Table 4, especially *K*, *Ca*, and *S*, and tool edge wear was found.

Table 3 shows values of the relatively corrosivity, R_w , evaluated from TGA plots, as shown in figures Figs. 6 to 10.

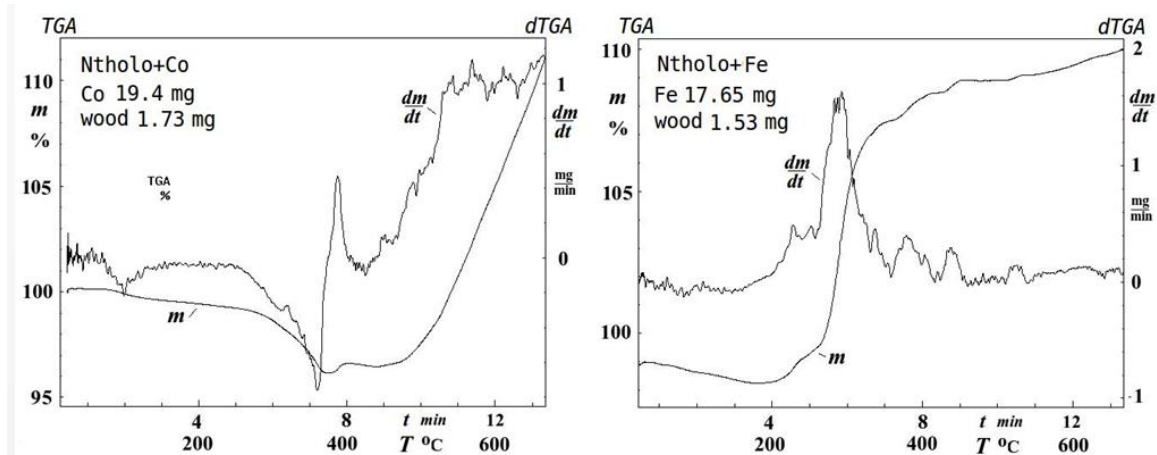


Fig. 6. Plots of TG (*m*) and dTG (*dm/dt*) for Co and Fe together for wood specimen Ntholo

It can be seen from these figures that in all wood specimens, the corrosion peaks were large. For *Co*, the largest corrosion peak was seen for Namuno wood (Fig. 7), 0.579 mg/min at a maximum temperature of 373 °C. With the exception of specimens of Metil wood, all of the HTC peaks for *Co* were seen at temperatures just after the maximum intensity of the thermal degradation of wood. For the *Fe* HTC peak, the largest corrosion peak was seen for Muanga wood (Fig. 8), at 2.33 mg/min at a maximum temperature of 288 °C. A very high corrosion peak was also observed for Namuno wood, at 2.294 mg/min at a maximum temperature of 279 °C.

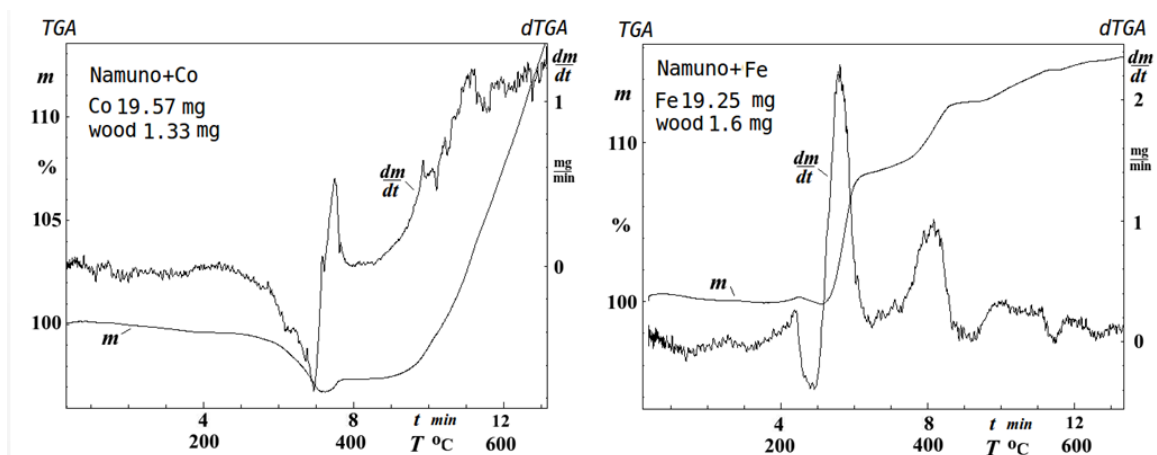


Fig. 7. Plots of TG (*m*) and dTG (*dm/dt*) for Co and Fe together for wood specimen Namuno

From X-Ray diffraction analyses performed in a previous work (Porankiewicz 2003b), it is known that the rapid mass increase (observed as a corrosion peak on the TGA

plot) was a result of the creation of an oxide phase of the metal (*Co*, *Fe*) specimens. The presence of such a metal oxide phase was not found before the corrosion peak appeared.

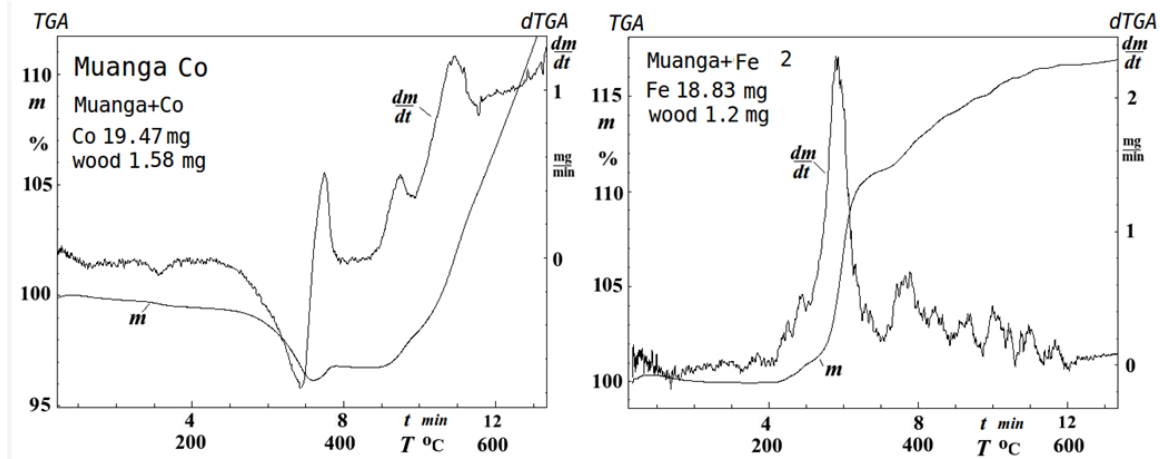


Fig. 8. Plots of TG (*m*) and dTG (*dm/dt*) for *Co* and *Fe* together for wood specimen Muanga

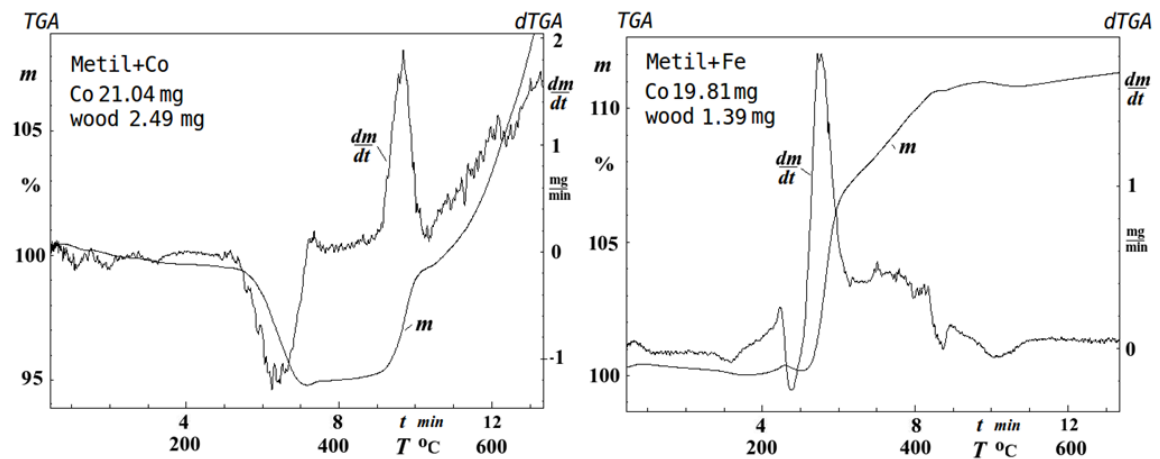


Fig. 9. Plots of TG (*m*) and dTG (*dm/dt*) for *Co* and *Fe* together for wood specimen Metil

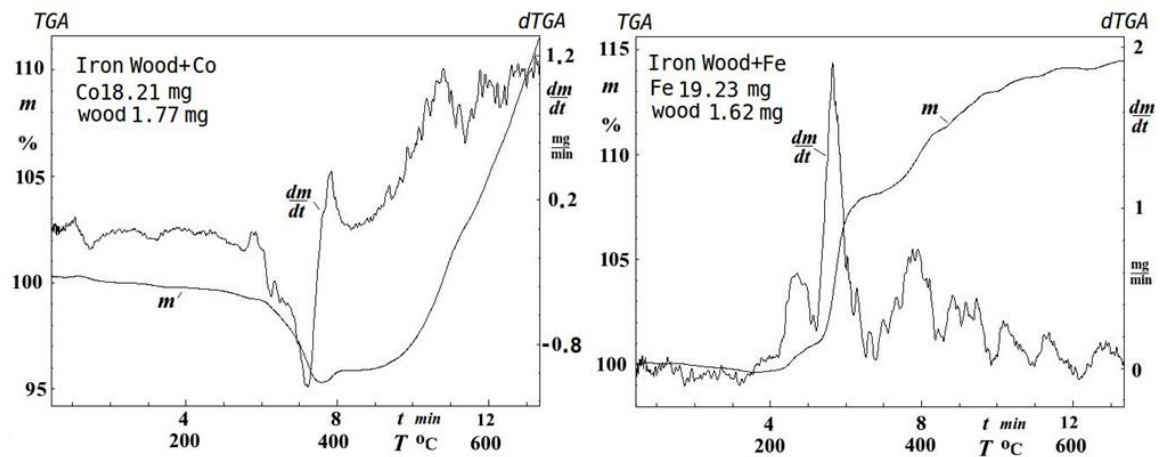


Fig. 10. Plots of TG (*m*) and dTG (*dm/dt*) for *Co* and *Fe* together for wood specimen Iron wood

The largest radius of edge round up, $\rho^{\circ} = 43 \mu\text{m}$, and the largest flank wear, $VB_{a}^{\circ} = 140 \mu\text{m}$, were observed for Ntholo wood (Table 2) and were associated with the highest HMC content, $CMC = 14524 \text{ mg/kg}$. The lowest observed radius of edge round up ($\rho^{\circ} = 5 \mu\text{m}$) and the lowest flank wear ($VB_{a}^{\circ} = 20 \mu\text{m}$) were not observed in the same wood species. The value of ρ° followed the value of VB_{a}° only for Ntholo and Muanga wood. The reason for this was asymmetrical abrasion of the rake and clearance surfaces, particularly due to the presence of damage on the cutting edge after milling Namuno and Metil wood. The lowest VB_{a}° , $20 \mu\text{m}$, was observed for $C_P = 2016 \text{ m}$, at low HMC and HTC (it would probably be of value $24 \mu\text{m}$ for the cutting path of $C_P = 4896 \text{ m}$, using power law interpolation). In case of the Namuno wood specimen, small flank wear was observed ($VB_{a}^{\circ} = 28 \mu\text{m}$) at the lowest HMC content, $CMC = 723 \text{ mg/kg}$ and largest HTC, $R_W = 5.09$. On the clearance surface of the tool after cutting the Ntholo wood specimen (Fig. 4a), a wide worn area with a corrosion pattern was seen. A similar but smaller worn area with corrosion patterns was seen on the clearance surface of the tool after cutting the Muanga wood specimen (Fig. 4c). These observations suggest that the combined influence of the HMC and the HTC caused these corrosion patterns. Small width of the visible worn area on the clearance surface of the tool after cutting Namuno wood (Fig. 4b) suggest a lower wearing effect which can be also associated with the lowest HMC. The worn area along the edge after cutting Metil wood (Fig. 4d) was almost invisible, but large scratches were seen. This suggests low abrasion and HTC effects but also suggests the presence of large-sized contaminant particles in the Metil wood specimen, but such large HMC particles were not found earlier (Table 3). It is recommended that a larger amount of Metil wood be examined in subsequent combustion analyses. All of the above remarks imply that the HMC probably plays a dominant role in cemented carbide blade wearing while milling the examined wood specimens.

The data in Tables 2 and 3 show that the HTC of wood toward Co , the binder in cemented carbide tool materials, as expressed relatively by the HTC quantifier R_W , was not well correlated with the observed tool wear rate. The HMC content and the HTC had overlapping effects for specimens 1 and 2. In this case, a synergistic effect of mechanical and HTC wear could take place. Although the densities differed very much, the observed edge wear and density were not correlated. Since no clear correlations between the observed edge wear, the HMC content, and the R_W and the wood density were seen, an attempt to use multi-parameter theoretical analysis, according to the work of Porankiewicz (2008), was performed. The theoretical model developed is described by Eqs. 3 to 15.

$$W^P = \sum_{i=1}^{ncp} \sum_{j=1}^{n\Phi} \sum_{k=1}^{nf} [\Delta\Delta_{ij} + \Delta W_{2ijk}] \quad (\mu\text{m}) \quad (3)$$

The predicted edge wear, W^P , as defined by Eq. 3 is the summation of the elementary wearing effects ΔW_{ij} and ΔW_{2ijk} along the cutting arc and the total feed path $F_{P1-4} = 406,355 \text{ mm}$ for specimens 1 to 4 and $F_{P5} = 167,323 \text{ mm}$ for specimen 5. The assumed number of fractions of the HMC was $n_f = 2$ ($f_1 = 1$ and $f_2 = 4$, as shown in Table 3). The cutting blade was moved for as many as $n_{cp} = 392,808$ steps for specimens 1 to 4 and $n_{cp} = 161,733$ steps for specimen 5, along the total feed paths F_{P1-4} or F_{P5} . The blade was moved along one single cutting arc of length 12.94 mm from beginning angle position $\phi_L = -0.00672 \text{ rad}$ to end position $\phi_U = 0.16134 \text{ rad}$ inside one feed step of $f_Z = 1.034 \text{ mm}$.

$$\Delta W_1 = \Delta w \cdot q_{dvb} \cdot q_{1R} \cdot q_{1D} \quad (4)$$

$$\Delta w_1 = e_1 \cdot C_{Pk}^{e_2} - e_1 \cdot (C_P - \Delta C_{Pk-1})^{e_2} \quad (5)$$

$$q_{dvb} = e_3 \cdot e_W^{-e_4 \cdot \ln(W) + e_5} \quad (6)$$

$$q_{1R} = 1 + e_7 \cdot R_W^{e_8} \quad \text{for } W^P > e_6 \quad (7)$$

$$q_{1D} = 1 + e_{14} \cdot D^{e_{15}} \quad (8)$$

$$\Delta w_{2f1} = w_{e2f1} \cdot S_{f1} \cdot q_{dvb} \cdot q_{2Rf1} \cdot q_{2D} \quad (9)$$

$$\Delta w_{2f2} = w_{e2f2} \cdot S_{f2} \cdot q_{dvb} \cdot q_{2Rf2} \cdot q_{2D} \quad (10)$$

$$q_{2Rf1} = 1 + e_{10} \cdot R_W^{e_9} \quad \text{for } W^P > e_6 \quad (11)$$

$$q_{2Rf2} = 1 + e_{11} \cdot R_W^{e_9} \quad \text{for } W^P > e_6 \quad (12)$$

$$q_{Sf1} = e_{12} \cdot f_1 \quad (13)$$

$$q_{Sf2} = e_{13} \cdot f_2 \quad (14)$$

$$q_{2D} = 1 + e_{16} \cdot D^{e_{17}} \quad (15)$$

where for the edge round up, $W^P = \rho^P$; for the flank wear, $W^P = VB_{\alpha}^P$; Δw_1 is the edge wear increase due to contact with wood; $w_{e2f1} \cdot S_{f1}$ and $w_{e2f2} \cdot S_{f2}$ are the wearing effects of a single HMC particle related from the position against the edge for fractions f_1 and f_2 , respectively; Δw_1 is the quotient of increase of the edge wear due to contact with wood; q_{dvb} is the quotient of decrease of the wear effect with an increase of the VB_{α}^P ; q_{1R} is the quotient of increase of the tool wear due to HTC expressed by R_W quantifier; q_{1D} is the quotient of increase of the tool wear due to wood density, D ; Δw_{2f1} and Δw_{2f2} are the edge wear increases because of contact with particles of mineral contamination for fractions f_1 and f_2 , respectively; q_{2Rf1} and q_{2Rf2} are the quotients of increase of the tool wear due to HTC, as expressed by the R_W quantifier, together with particles of HMC of fractions f_1 and f_2 , respectively; q_{2D} is the quotient of increase of the tool wear due to wood density, D , together with particles of HMC; and $e_W = 2.7182818$.

For ρ^P , the quality of approximation reached was as follows: $R^2 = 0.93$, and $S_R = 11.6$. For VB_{α}^P , the quality of approximation reached was as follows: $R^2 = 0.94$, and $S_R = 168.5$. The reason for such discrepancies could be inaccuracies in a LM measurement of an edge dullness parameter (ρ or VB_{α}) or in the evaluation of the HMC content. It must be noted that the values of the observed edge recession along the clearance surface, VB_{FC} , given in the work of Cristóvão *et al.* (2010) for specimens 1 to 5 did not allow reasonable theoretical simulation results ($S_R > 1400$). Graphical illustrations of the relationships between ρ^P and $VB_{\alpha}^P = f(D, C_{MC})$ are shown in Fig. 11.

The maximum synergistic effect of the C_{MC} of the particles of fraction f_1 and the HTC effect, as expressed by the R_W quantifier evaluated in Fig. 11, reached as high as 96%. The wearing effect of the HTC itself appeared to be the dominant factor influencing cemented carbide blade dulling in the examined cases. The role of C_{MC} itself was lower and the effect of the D was the lowest. For the lowest R_W and the C_{MC} and the largest D , after a cutting path of $C_P = 5082$ m, the predicted ρ^P and VB_{α}^P values reached 3 and 14 μm , respectively.

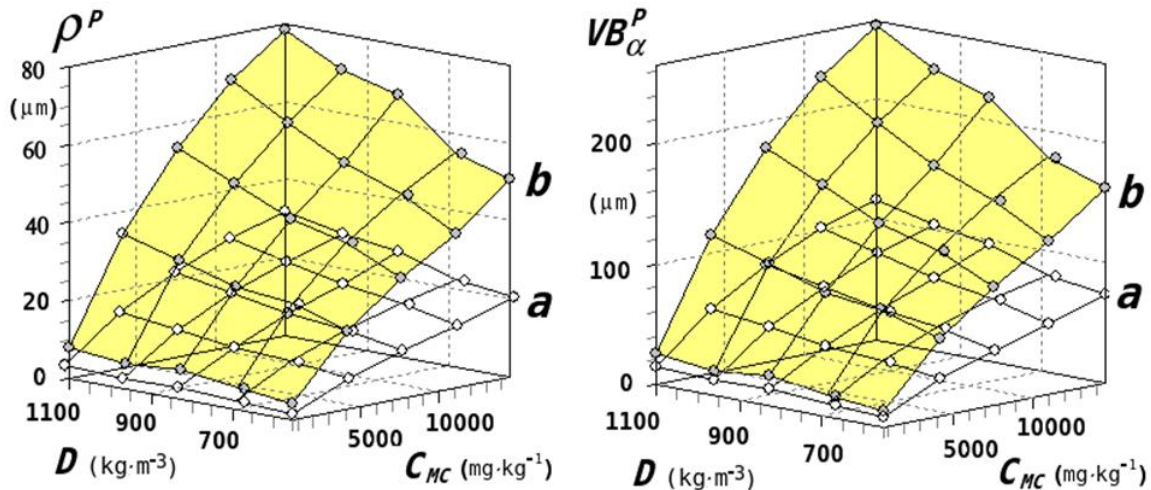


Fig. 11. Plots of relationships between wood density, D , and the HMC content, C_{MC} and predicted: edge round up, ρ^P ; flank wear, VB_{α}^P ; for: a - $R_W = 1.0$ and b - $R_W = 5.09$; $C_P = 5082$ m; $S_{MC} = 25$ μm

Theoretical simulation performed for the flank wear, VB_{α}^P , with other kinds of quantifiers describing the HTC, was evaluated on basis: all of the corrosion peaks, R_{mx} ; summation of area, A , of all corrosion peaks, R_A ; weighted average quantifier, R_{mTA} , containing maximum temperature, T_x , in corrosion peaks and the range of the temperatures of the corrosion peaks, dT_x , and corrosion peaks area, A ; weighted average quantifier with ranks, R_{mTar} ; were unable to obtain better approximation than one with the R_x quantifier. The quantifiers R_{mx} , R_A , and R_{mTa} were examined in previous works (Porankiewicz *et al.* 2003; Porankiewicz *et al.* 2006; Porankiewicz 2008) in relation to HSS cutting tools.

CONCLUSIONS

1. The Ntholo wood specimen was most hard mineral-contaminated with $C_{MC} = 14524$ mg/kg and particle sizes smaller than 25 μm .
2. A wide worn area with corrosion patterns on the clearance surface of the tool after cutting Ntholo wood was explained by a combined effect of the hard mineral contamination and high temperature corrosivity.
3. The results of the theoretical simulation performed show that the most influencing factor on cemented carbide tool wear was the high temperature corrosivity, together with the hard mineral contaminant content, which had a maximum synergistic effect as high as 95%.
4. The relative quantifier of high temperature corrosivity, R_W , based on the average value of the corrosion peaks observed on the TGA plots just the after maximum wood mass degradation rate, provided the best fit between the observed and predicted tool wear values in the theoretical simulation performed.
5. The sizes of rounded, small, hard mineral contamination particles can be measured using SEM images of remainings on Whatman glass filters.

6. Spectroscopy methods such as EDAX and AAS seem unsuitable for the evaluation of the hard mineral contaminant content, C_{MC} , in wood specimens with respect to tool wear.

ACKNOWLEDGMENTS

The authors are grateful for the support of the PCSS, Poznań, Poland for a calculation grant.

REFERENCES CITED

- Cristóvão, L., Grönlund, G., Ekevad, M., Siteo, R., and Marklund, B. (2009). "Brittleness of cutting tools when cutting ironwood," in: *19th Int. Wood Mach. Sem.*, Nanjing.
- Cristóvão, L., Lhate, I., Grönlund, A., Ekevad, M., and Siteo, R. (2011). "Tool wear for lesser-known tropical wood species," *Wood Mat. Sci. Eng* 6(3), 155-161. DOI: 10.1080/17480272.2011.566355.
- Darmawan, W., Rahayu, I., Tanaka, C., and Marchal, R. (2006). "Chemical and mechanical wearing of high speed steel and tungsten carbide tools by tropical woods," *J. Trop. For. Sci.* 18(4), 255-260.
- Porankiewicz, B. (2014). "Wood machining investigations: Parameters to consider for thorough experimentation," *BioResources* 9(1), 1-3. DOI: 10.15376/biores.9.1.4-7
- Porankiewicz, B. (2003a). "A method to evaluate the chemical properties of particle board to anticipate & minimize cutting tool wear," *Wood Sci. and Tech.* 37(1), 47-58. DOI: 10.1007/s00226-003-0166-8
- Porankiewicz B. (2003b) "*Tępienie się ostrzy i jakość przedmiotu obrabianego w skrawaniu płyt wiórowych [Cutting edge blunting & quality of the working element in particle board cutting]*," Printing House of Agricultural Univ. of Poznań, Habilitation Works, Poznań, Poland, pp. 341.
- Porankiewicz, B. (2008). "Theoretical method for prediction of the cutting edge recession during milling wood and secondary wood products," *BioResources* 3(4), 1103-1117.
- Porankiewicz, B., Iskra, P., Sandak, J., Tanaka, J., and Józwiak, K. (2006). "High speed steel tool wear after wood cutting in presence of high temperature and mineral contamination," *Wood Sci. & Tech.* 40, 673-682. DOI: 10.1007/s00226-006-0084-7
- Porankiewicz, B., Sandak, J., and Tanaka, C. (2005). "Factors influencing steel tool wear when milling wood," *Wood Sci. and Tech.* 39(3), 225-234. DOI: 10.1007/s00226-004-0282-0
- Porankiewicz, B., Iskra, P., Józwiak, K., Tanaka, C., and Zborowski, W. (2008). "High speed steel tool wear after wood milling in presence high temperature tribochemical reactions," *BioResources* 3(3), 838-859. DOI: 10.15376/biores.3.3.838-858
- Staniszewski, J., and Porankiewicz, B. (1978). "*Kryteria i metody oceny stopienia narzędzi skrawających do obróbki drewna [Criteria and blunting assessment methods of wood cutting tools]*," Printing House of Agricultural Univ. of Poznań, Poznań, Poland, pp. 57.

Article submitted: April 8, 2015; Peer review completed: June 20, 2015; Revised version received: Nov. 2, 2015; Accepted: Nov. 7, 2015; Published: November 24, 2015.
DOI: 10.15376/biores.11.1.585-598

APPENDIX

The following estimators for Equations 3 to 15 for the edge round up, ρ^O , were evaluated: $e_1 = 2.94776 \cdot 10^{-5}$; $e_2 = 5.43699 \cdot 10^{-3}$; $e_3 = 4.50867 \cdot 10^{-5}$; $e_4 = 6.85641 \cdot 10^{-3}$; $e_5 = 6.97489 \cdot 10^{-2}$; $e_6 = 5.5911$; $e_7 = 0.57998$; $e_8 = 0.86285$; $e_9 = 0.71746$; $e_{10} = 2.362887$; $e_{11} = 0.46051$; $e_{12} = 0.55724$; $e_{13} = 0.97752$; $e_{14} = 1.65125 \cdot 10^{-2}$; $e_{15} = 9.91695 \cdot 10^{-3}$; $e_{16} = 8.76272 \cdot 10^{-2}$; and $e_{17} = 0.13401$. Rounding the values of the estimators for each Equation to 6 decimal places yielded acceptable deterioration of fit of less than 1%. Reducing the number decimals to 5, 3, or 2 caused unacceptable deterioration of fit by as much as 96 and 108%, respectively.

The following estimators for Equations 3 to 15 for the flank wear, VB_{α}^O , were evaluated: $e_1 = 9.83182 \cdot 10^{-6}$; $e_2 = 8.9264 \cdot 10^{-4}$; $e_3 = 5.31132 \cdot 10^{-5}$; $e_4 = 3.80234 \cdot 10^{-3}$; $e_5 = 7.05214 \cdot 10^{-3}$; $e_6 = 6.45928$; $e_7 = 0.5719$; $e_8 = 0.76568$; $e_9 = 0.43094$; $e_{10} = 3.01585$; $e_{11} = 0.91149$; $e_{12} = 1.17249$; $e_{13} = 2.14328$; $e_{14} = 1.43351 \cdot 10^{-2}$; $e_{15} = 3.30962 \cdot 10^{-2}$; $e_{16} = 0.22752$; and $e_{17} = 0.17442$. Rounding the values of the estimators for each Equation to 6 decimal places yielded acceptable deterioration of fit of less than 1%. Reducing the number decimals from 5 to 2 caused unacceptable deterioration of the fit by as much as 270%.